JOURNAL OF GEOPHYSICAL RESEARCH, VOL. 98, NO. C8, PAGES 14,423–14,435, AUGUST 15, 1993

A Chlorofluoromethane and Hydrographic Section Across Drake Passage: Deep Water Ventilation and Meridional Property Transport

WOLFGANG ROETHER, REINER SCHLITZER, ALFRED PUTZKA, PETER BEINING, AND KLAUS BULSIEWICZ

Universität Bremen, Bremen, Germany

GERD ROHARDT

Alfred-Wegener-Institut für Polar- und Meeresforschung, Bremerhaven, Germany

FRANK DELAHOYDE

Oceanographic Data Facility, Scripps Institution of Oceanography, La Jolla, California

New hydrographic and nutrient data obtained on a section across Drake Passage (F/S *Meteor* January 1990, World Ocean Circulation Experiment Hydrographic Program section S1) are in close agreement with property sections reported previously. The chlorofluoromethanes CFM 11 and CFM 12 were measured in Drake Passage for the first time. CFM concentrations are found to decrease from the surface down into the Upper Circumpolar Deep Water, for which they confirm water renewal from the south. For the Lower Circumpolar Deep Water, in which CFM concentrations were above detection limit only south of the Polar Front, very little water renewal on the CFM time scale is implied. Nonvanishing CFM is again found in the Weddell Sea Deep Water and the Southeast Pacific Deep Water toward the bottom in the south, but recent ventilation for the latter water mass is rejected. CFM 11 and CFM 12 concentrations vary essentially in constant proportion down to very low concentrations, questioning the possibility of using CFM ratios as "age" markers. The observed ratios are shown to be a natural feature of the upwelling regime of the southern ocean. Property concentrations on isopycnal surfaces display large undulations, reaching down into the Upper Circumpolar Deep Water. Their extrema, due to varying contribution of young water of southern origin, are situated at the boundaries of the current bands of the Antarctic Circumpolar Current. The feature is ascribed to property advection by rings and is taken to support previous claims that rings are an important transport mechanism across the Antarctic Circumpolar Current and that they might assist in maintaining its fronts.

1. INTRODUCTION

Drake Passage acts as the principal water source for the Atlantic sector of the world ocean, by allowing Pacific waters to be injected by the Antarctic Circumpolar Current (ACC). It has a layered water mass structure, as described in detail by *Sievers and Nowlin* [1984] on the basis of hydrographic and nutrient distributions. The most extensive water mass is the Circumpolar Deep Water (CDW). Noticeable water renewal, fed from sources in the south, occurs in its upper portion (UCDW) and in the waters further up, as well as in a water mass present at the base of the southern continental slope of the passage (Weddell Sea Deep Water or WSDW). The UCDW at the same time shows characteristics derived from mid-depth waters of the Indian-Pacific sector. The lower portion of the CDW (LCDW) carries a salinity signal ultimately derived from the North Atlantic Deep Water, and is regarded as a major water source for the Weddell Sea [*Reid et al.*, 1977; *Whitworth and Nowlin*, 1987].

Water masses slope upward toward the south, and the corresponding change of water characteristics across the ACC along isobars is concentrated in distinct fronts [*Sievers and Nowlin*, 1984]. Much of the flow of the ACC is concentrated in the fronts, the primary ones being the Subantarctic Front (SAF) and the Polar Front (PF) [*Emery*, 1977], which act as the principal boundaries of Subantarctic and Antarctic waters [*Nowlin and Klinck*, 1986]. In Drake Passage, coastal waters to the south are separated by a further front, the Continental Water Boundary (CWB) [*Sievers and Nowlin*, 1984]. There are, consequently, north-south changes in water mass characteristics, partly in relationship to the fronts, but by and large, water masses appear to be laterally coherent across the passage [*Sievers and Nowlin*, 1984].

Meanders and (mostly cold-core) rings, caused by dynamic instability of the frontal jets of the ACC, have been observed and studied, in particular in Drake Passage [*Hofmann and Whitworth*, 1985; *Nowlin and Klinck*, 1986]. It has been suggested that cold-core rings shed from the PF have a tendency to show up attached to the SAF [*Sievers and Emery*, 1978; *Sievers and Nowlin*, 1984; *Lutjeharms and Valentine*, 1984]. Claims have been made that rings effect property transport across the ACC [*Bryden*, 1983] and that they might help in maintaining the fronts [*Lutjeharms*, 1989]. Theoretical guidance on their behavior is sparse, as existing ring studies [*Stern and Flierl*, 1987; *Smith and Davis*, 1989; *Brickman and Ruddick*, 1990] do not deal with the ACC situation, and numerical modeling studies still lack adequate horizontal resolution [*Webb et al.*, 1991].

Water mass renewal is a subject suitable for ocean tracer studies, involving in particular transient tracers [*World Climate Research Program (WCRP)*, 1988*b*]. Renewal by surface waters is often termed "ventilation", reflecting the fact that many tracers are delivered from the atmosphere in gaseous form. For the Drake Passage area, available transient tracer information is sparse; tritium data, from the Geochemical Ocean Sections (GEOSECS) program [*GEOSECS*, 1987], are limited in number, and as

Paper number 93JC00786.
0148-0227/93/93JC-00786$05.00

concentrations are low and measurements were done by counting, relative errors are large. Significant concentrations were only found down to about 400-m depth. The only transient tracer data available in deep water appear to be observations of the chlorofluoromethane CFM 11 in the WSDW east of Drake Passage [*Nowlin and Zenk*, 1988].

Ocean tracer work was part of a Drake Passage hydrographic section completed recently by F/S *Meteor* (cruise 11, leg 5, January, 1990). The section represented section S1/A21 of the World Ocean Circulation Experiment (WOCE) Hydrographic Program (WHP) and covered the full suite of WHP parameters [*WCRP*, 1988*a*]. In the present communication we report hydrographic, silica, and chlorofluoromethane (CFM) observations that were obtained. We compare the water mass distribution found in the *Meteor* data with previous work [*Sievers and Nowlin*, 1984] and we explore the information content of CFM data complementing classical hydrography. We start with a brief description of CFMs as ocean tracers, followed by an outline of *Meteor* procedures. Subsequently, the *Meteor* hydrographic data are presented and analyzed. CFM data are then considered and are found to contain definite information on ventilation of the deep water masses. Observed concentration ratios of CFM 11 and CFM 12 are shown to be a natural result of the upwelling of southern ocean waters. A final topic is isopycnal distributions, which appear to be highly structured; they confirm the ventilated waters to come from the south, and reemphasize the role of rings.

2. CHLOROFLUOROMETHANES AS TRACERS

The anthropogenic chlorofluoromethanes CFM 11 ($CClF_3$) and CFM 12 (CCl_2F_2) in ocean surface waters attain near-solubility-equilibrium values [*Warner and Weiss*, 1985] with atmospheric concentrations [*Gammon et al.*, 1982]. Their delivery began in the 1940s and produced steadily increasing environmental concentrations, such that CFM 11 to CFM 12 ratios also increased up to about 1975 but then leveled off (Figure 1). CFM concentrations of waters equilibrated with a given atmospheric concentration depend strongly on the temperature of the water [*Warner and Weiss*, 1985]. It is therefore convenient to convert measured concentrations to an equivalent solubility-equilibrium partial pressure in air (in parts per trillion by volume, pptv), if CFM values in waters of different temperature are to be compared.

CFM concentrations in subsurface waters reflect addition of surface waters, or ventilation, during the past decades. Substantial subsurface concentrations indicate recent or strong addition, and vanishing CFM concentrations exclude significant addition on the CFM time scale (Figure 1). In this sense, waters may be characterized as "young" (rapidly ventilated) or "old" (slowly ventilated) on the basis of their CFM concentrations. In quantitative terms, if ocean mixing was sufficiently small, CFM concentrations would essentially be preserved along trajectories of flow from the surface layer into the interior ("piston flow"). In this hypothetical case, a measured subsurface concentration, or

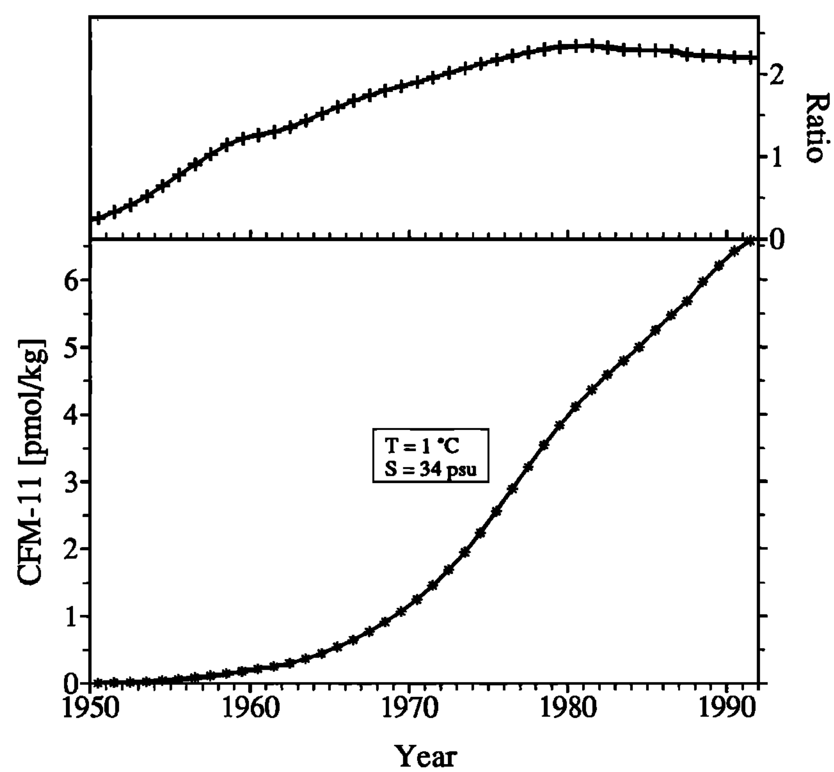

Fig. 1. (Bottom) CFM 11 concentration and (top) CFM 11 to CFM 12 concentration ratio for southern ocean surface waters, 1950-1991. The curves represent values for water of 1°C and 34 psu in equilibrium [*Warner and Weiss*, 1985] with atmospheric concentrations for Cape Grimm, Tasmania (P. Salameh and R. Weiss, Tables of reconstructed atmospheric F-11 and F-12 histories, unpublished note, Scripps Institution of Oceanography, 1992), but with CFM 11 corrected by a factor of 1.03 (section 3). Per degree temperature increase, CFM 11 concentrations (ratios) would decrease by about 6 (0.8)%.

ratio, could be converted into time since the water left the surface layer, simply by comparison with the surface water CFM time histories (Figure 1). In reality, mixing affects CFM distributions by producing large deviations from a piston flow situation, as will be seen below (section 5).

One case considered and applied to the WSDW is admixture of low-CFM water to a flow of younger water. Because the ratio of a mixture is biased toward those of the high concentration, i.e., young, components, an observed ratio, by comparison with Figure 1, will give an upper limit of an advective transit time, and observed concentration a lower limit of dilution [*Weiss et al.*, 1985; *Pickart et al.*, 1989]. The other case is one believed to be characteristic of the southern ocean [*Gordon and Taylor*, 1975], namely, a situation of upwelling of low-CFM water with superimposed admixture of younger waters from above. Because of the bias mentioned, ratios in this case must be expected to remain high relative to Figure 1 toward low concentrations. This case is applied below to the depth range of pronounced CFM decline below the surface layer.

Mean subsurface residence times are large for most Drake Passage deep water masses, as demonstrated, for example, by their low ^{14}C contents [*Stuiver et al.*, 1983]. The ^{14}C distribution, however, does not exclude significant contributions of young water, as concentrations in the entire deep circumpolar ocean are quite near to concentrations in the potential source waters [*Stuiver et al.*, 1983]. To find such contributions, CFM observations are a useful tool. For a quantitative assessment, however, the time delay between the actual ventilation process and the arrival of the ventilated water at the point of observation must be taken into account. For example, if the transit time is known to be at most 20 years, and if CFM 11 observations in 1990 give an upper limit of 0.025 pmol/kg for a water mass, then according to Figure 1 (post-1970 surface water concentration > 1.4 pmol/kg) a maximum contribution of such ventilated water of about 2% (0.025/1.4 = 0.018) is provided. This indicates that quite small contributions are detectable in principle. However, as transit time information is not at hand, we restrict ourselves below to reporting upper limits of CFM concentration for the "oldest" water masses.

3. Data Collection and Measurement

Meteor cruise 11, leg 5 (Ushuaia-Cape Town, January 23 to March 8, 1990) started the field phase of the WHP with a one-time survey section across Drake Passage [*Roether et al.*, 1990]. The section was placed west of the classical ones [*Sievers and Nowlin*, 1984], in order to avoid possible disturbance of water masses by bottom topography in the passage (Figure 2). Sixteen stations were occupied, at 30-n.mi (56 km) nominal spacing (Figure 2). Due to winch problems, the ship turned back at the southern end of the section, which gave opportunity for fill-in work at the positions of stations 115, 113, and 106. Only bottle data are considered in the present paper.

Basic instrumentation was a 24 x 12-L rosette (General Oceanics) and a Mark IIIB conductivity-temperature-depth profiler (CTD) (Neil Brown), with sensors calibrated at Scripps Institution of Oceanography (SIO) Oceanographic Data Facility (ODF) prior to and after the cruise. Stability of the temperature and pressure sensors was monitored with digital reversing thermometers and pressure gauges (SIS). Accuracy in temperature is estimated to be ±0.002 K. Salinity was measured using an Autosal instrument with an estimated accuracy of 0.003 psu (practical salinity units). Nutrients and dissolved oxygen were determined using Scripps ODF techniques. Data

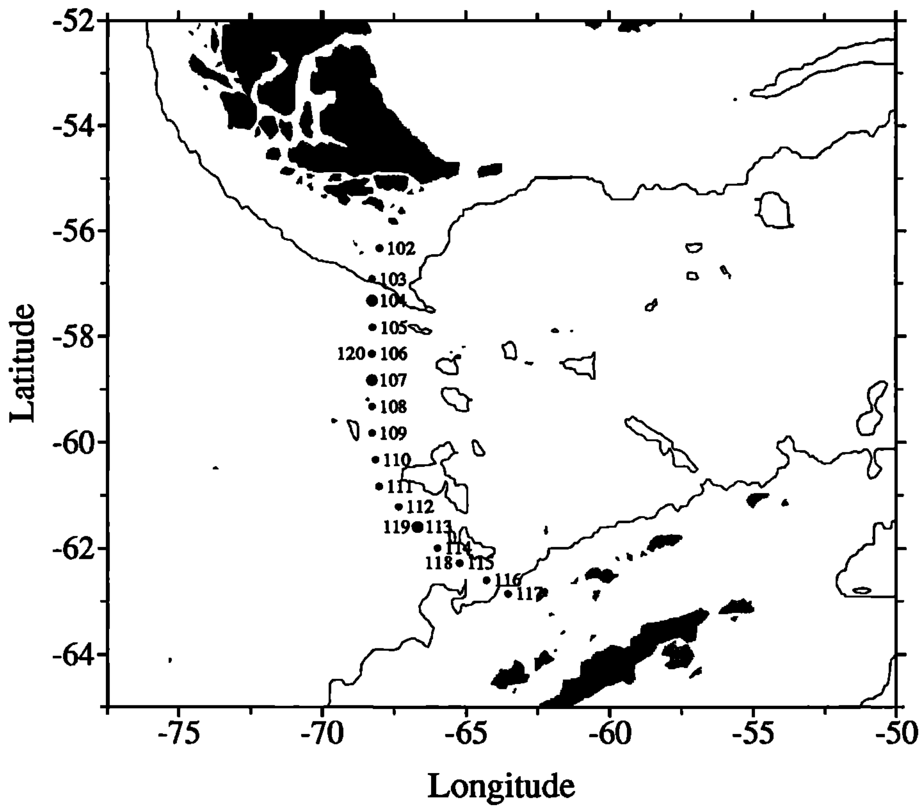

Fig. 2. Stations of Drake Passage section *Meteor* cruise 11/5, January 1990 (WHP S1/A21; large dots indicate large-volume stations). Depth contour shown is 3000 m.

quality was monitored by cross checking the independent measurements for consistency, which led to rejection of samples in just a few cases.

The CFM measuring unit used was a fully automated version of the *Bullister and Weiss* [1988] design. Samples were taken in the usual way using glass syringes. Gas standard runs and water line blanks were run approximately bihourly, and full calibration runs were done repeatedly. To check for the overall blank, a special cast was made into supposedly CFM-free water. It was found that this blank was indistinguishable from the water line blank. This showed that a sampling blank was negligible within errors. Taking into account the uncertainty of this blank, as well as sample replica precision and calibration uncertainty (from gas standard and calibration runs, including their drift), we find the total 1-σ data error to be $\pm 2\%$ or 0.01 pmol/kg (whichever is greater), for both CFMs 11 and 12. This converts to a precision in CFM 11 to CFM 12 ratio of $\pm 3\%$ at sufficiently large concentrations. The highest CFM 11 concentrations unfortunately were outside the calibration range (by at most 40%). The added uncertainty due to the extrapolation was estimated to be $\pm 2\%$ for the maximum CFM 11 concentrations observed (about 6 pmol/kg), for which the total error thus becomes $\pm 3\%$. The detection limit is taken to be 0.01 pmol/kg in CFM 11. A few outliers (on the basis of being outside the correlation with other properties) were removed. The CFM data are reported on the SIO 1986 scale ($\pm 0.3\%$; the compressed-air gas standard used for calibration at sea was measured, after the cruise, against gas standards provided by R. F. Weiss, SIO). We note that a few measurements of CFM 11 in air taken on the cruise somewhat exceeded the published tropospheric record for the region (Figure 1). This excess is taken to support the calibration, however, as similar excesses (about 3%) were found on subsequent cruises and have likewise been reported by *Doney and Bullister* [1992].

4. HYDROGRAPHIC DISTRIBUTIONS

Meteor hydrographic observations are presented and are compared with those in the classical description of *Sievers and Nowlin* [1984], from which work (hereinafter referred to as SN84) we also accept definitions and nomenclature. Densities at water mass boundaries and some water mass characteristics according to the SN84 analysis are listed in Table 1.

Figure 3 gives *Meteor* sections of potential temperature, salinity, oxygen, silicate, and density, and Figure 4 presents the

TABLE 1. Characteristics of Water Masses and Densities at Water Mass Boundaries in Drake Passage as given by *Sievers and Nowlin* [1984]

Water Mass[a]	Density[b] at Upper Boundary	Water Mass Characteristic or Comment
AAIW	27.2	joins WW south of PF
UCDW	27.3-27.5	density rises south of PF, oxygen minimum core
LSDW	36.98/27.77	density somewhat uncertain[c], salinity maximum core
SEPDW	46.0	silica maximum > 135 µmol/kg
WSDW	46.04	

[a] Water masses are defined in text.

[b] Density may be σ_0, σ_2, σ_4 depending on depth (see Figure 3e).

[c] An approximate average density corresponding to the characterization offered by SN84 for this boundary is listed.

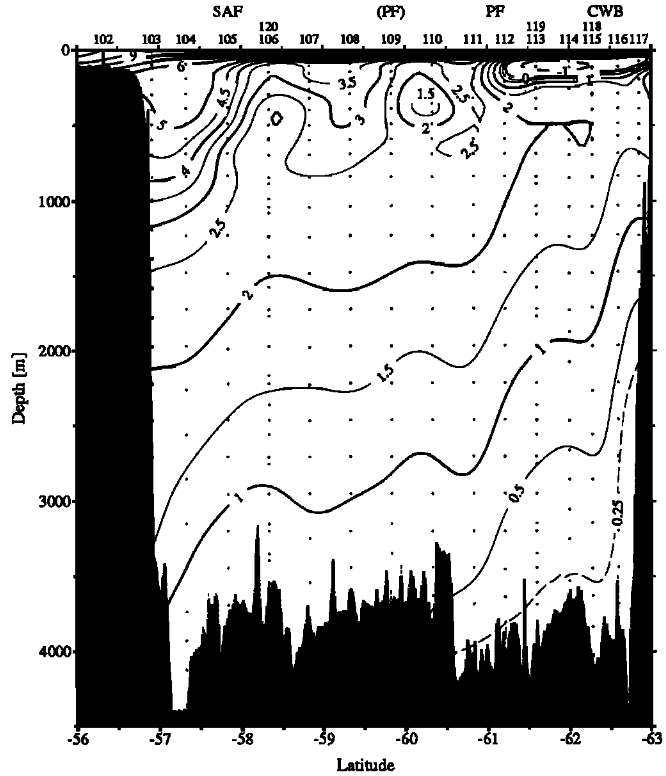

Fig. 3a. *Meteor* potential temperature section across Drake Passage. Station numbers (Figure 2) and positions of the fronts (Figure 4) are indicated; bottom depth is from ships' recordings. Isolines were obtained by objective interpolation between data points (dots) with variable correlation length, excessive smoothing was avoided.

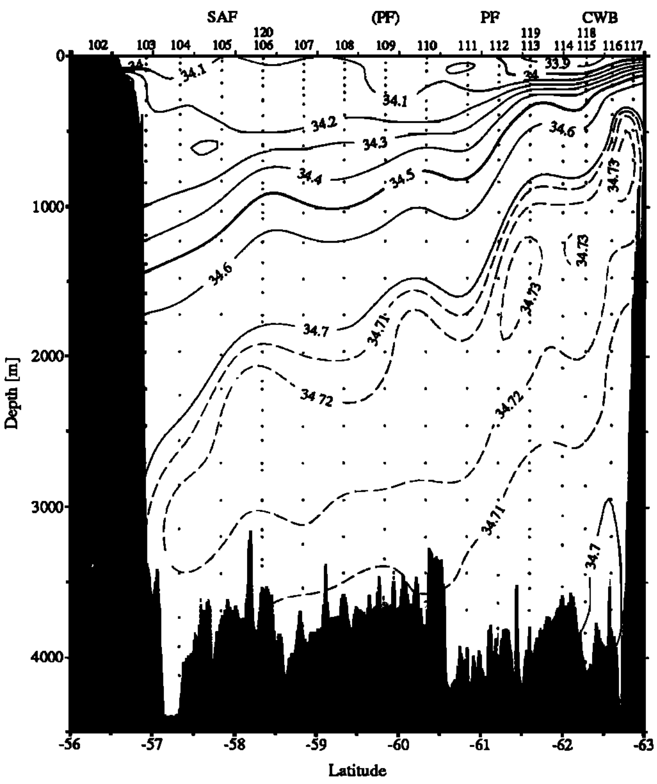

Fig. 3b. Same as Figure 3a, for salinity (practical salinity units).

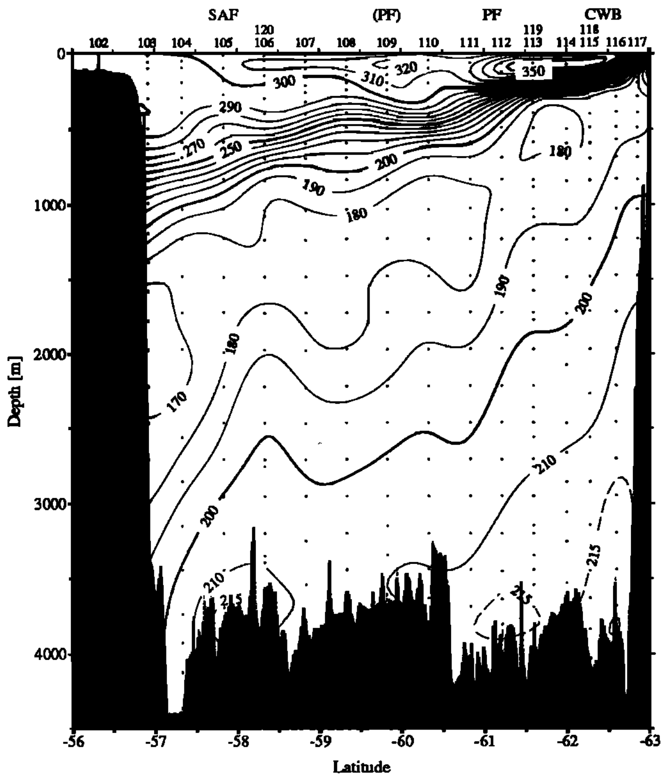

Fig. 3*c*. Same as Figure 3*a*, for oxygen (micromoles per kilogram).

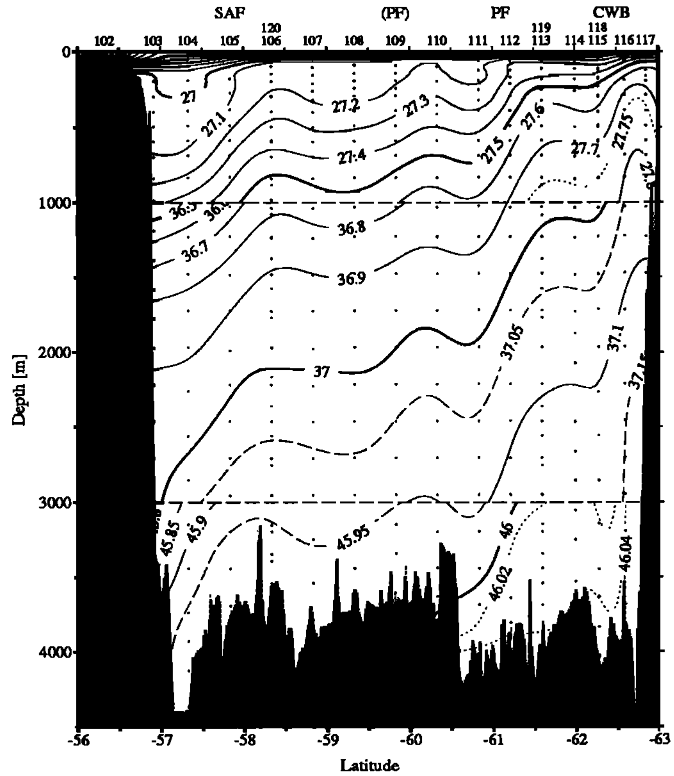

Fig. 3*e*. Same as Figure 3*a*, for density parameter, σ_0 (0-1000 m), σ_2 (1000-3000 m), σ_4 (3000 m to bottom).

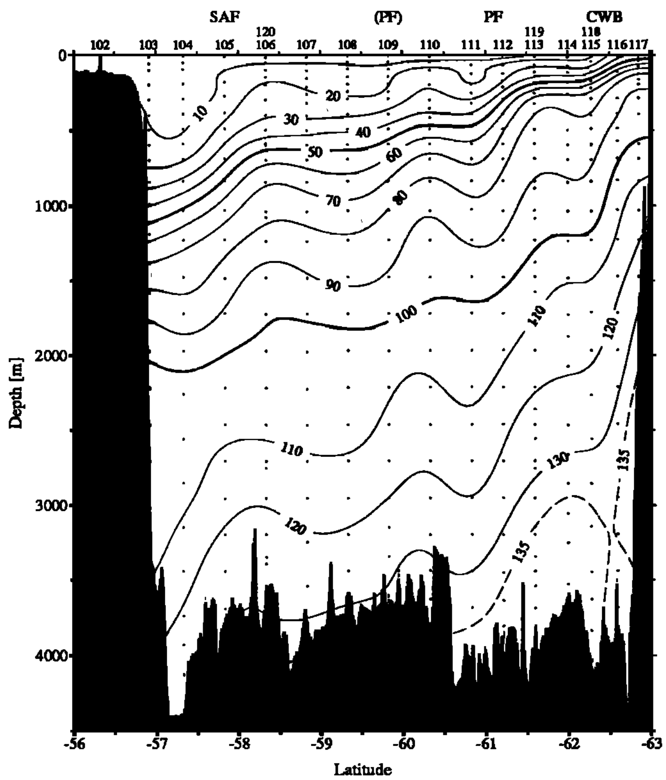

Fig. 3*d*. Same as Figure 3*a*, for silica (micromoles per kilogram).

geostrophic velocity field. Temperature (Figure 3*a*) shows the characteristic southward rising of isolines, which is concentrated in fronts, the positions of which are indicated in Figure 3. Apart from the SAF, the PF, and the CWB, there is an additional current band (Figure 4) near 60°C associated with a sharp rise of the 2.5°C isotherm and a temperature minimum (near station 110). The current band is therefore believed to be a secondary Polar Front feature, similar to previous observations [SN84, Figure 4]. Over most of the water column, the *Meteor* and SN84 sections are strikingly similar. In Figure 3*a* the shallow subsurface temperature minimum of the Winter Water (WW) is clearly present south of the PF (Figure 3*a*), and the temperature range and form of isolines through the water column are very near to those in SN84. The salinity section (Figure 3*b*) is similar, particularly in the extent and salinity value of the deep salinity maximum that represents the core of the LCDW (Table 1), even to the degree that values exceeding 34.73 appear only south of the PF, at which front, furthermore, a distinct depth change is apparent. Similar agreement is noted for the oxygen minimum layer (Figure 3*c*), which characterizes the UCDW, including southward shrinking stepwise at the PF and CWB. The WW shows maximum oxygen concentrations. Likewise, the silica distribution (Figure 3*d*) resembles that of oxygen, e.g., in the depths, and in the depth increases at the CBW and the PF, of the 100- and 130-µmol/kg silica isolines.

Differences between the *Meteor* and SN84 sections are apparent in the deepest layers and presumably are due to the more westerly track of the *Meteor* relative to the previous work (Figure 2) discussed in section 3. Oxygen concentrations (Figure 3*c*) at the ocean floor in the northern part of the passage appear to be higher than found previously, conceivably because of less mixing of low-oxygen water from above. In the southern part, the layer that has silica concentrations >135 µmol/kg (Figure 3*d*) is not separated from the ocean floor nor the southern continental rise of the passage. The silica maximum is related to the eastwardly flowing Southeast Pacific Deep Water (SEPDW; Table 1). SEPDW receives its characteristics by Antarctic water

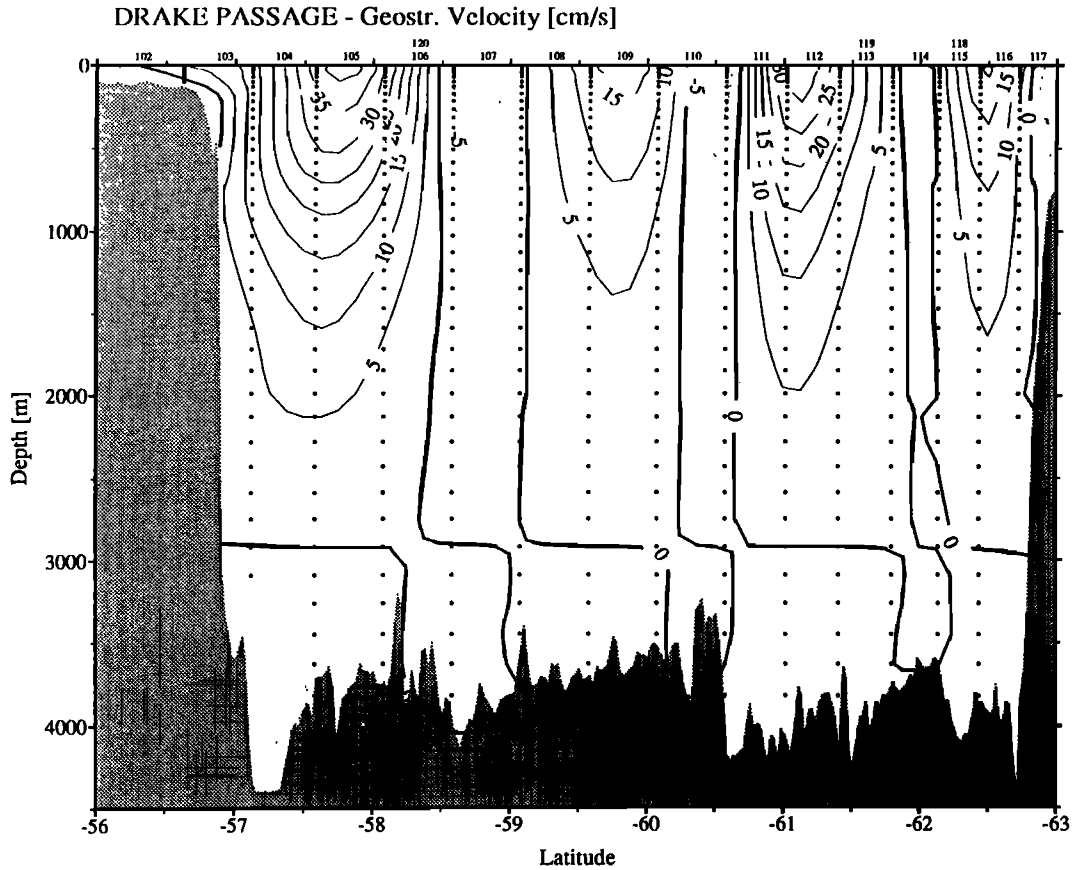

Fig. 4. Isolines of *Meteor* geostrophic velocity, relative to 3000 dbar. Fronts (Figure 3) were identified with positions of maximum velocities of the four current bands indicated.

mass conversion somewhere in the Indian-Pacific sector (SN84) and in Drake Passage adjoins WSDW (Table 1, Figure 3*e*), which originates in the Weddell Sea and spreads westward along the southern continental slope [*Nowlin and Zenk*, 1988]. Therefore a reasonable explanation of the finding is reduced presence of WSDW on the *Meteor* section. The PF on the *Meteor* track was encountered quite far south. Southward displacement of the PF toward the west in Drake Passage is known to occur, but the position actually found is almost 100 n.mi (185 km) even further south than expected according to the maps of *Sievers and Nowlin* [1988]. A consequence is that the deepest water masses (SEPDW and WSDW), which by their densities (Table 1) appear to be restricted to south of the PF (Figure 3*e*), have a limited extent along the *Meteor* section.

In the upper waters, the temperature section (Figure 3*a*) displays some undulating features (centered near stations 106/120, 110, and possibly 114) which are absent in the SN84 distributions. The middle one appears to be related to the mentioned secondary PF, distinguishing this front from the one observed by SN84, which resembled a weakened, but steady, extension of the temperature minimum related to the WW. It appears that the positions of the undulations coincide with those of current reversals in Figure 4. We also note that in the velocity field (Figure 4), countercurrents are present on the southern margins of all four current bands. Such countercurrents have been repeatedly found previously, both in observations [*Nowlin et al.*, 1977; *Sievers and Nowlin*, 1984] and in numerical model output [*Webb et al.*, 1991; D. Wolf-Gladrow, Bremerhaven, private communication, 1992].

5. CFM Distribution and Ventilation

The Drake Passage CFM 11 section is presented in Figure 5. CFM concentrations are maximal in near-surface waters, and decrease steadily downward to the detection limit concentration (0.01 pmol/kg) in about 1000 to 2500 m depth. Nonvanishing concentrations are again found in a deep core in the south. In between there is a wedge of water with nondetectable CFM 11 that separates from the bottom toward the southern continental slope. Undulation of the CFM 11 isolines in the upper 1000 m correlates with the temperature features near stations 106/120, 110, and 114 noted above. This intriguing correlation is addressed below. The general slope toward the south of CFM 11 isolines in the upper layers evidently deviates from that for density (Figure 3*e*), more so than is found for other properties (Figures 3*b*, 3*c*, and 3*d*). In the following we discuss the CFM distribution in the context of water masses and their ventilation.

The deep CFM 11 core in the south (Figure 5) is related to the WSDW and the SEPDW. Their water mass boundary (Table 1, Figure 3*e*) approximately corresponds to the 0.05-pmol/kg CFM 11 isoline. The mean values for CFM 11 concentration and concentration ratio for the four data points within the deep 0.1-pmol/kg contour are 0.17 pmol/kg and 2.0. This concentration in the core of the WSDW is markedly lower than values observed during AJAX in 1983-1984 in the WSDW core at the northern side of the South Scotia Ridge at 56° W and 48° W, i.e., exceeding 0.4 and 0.6 pmol/kg, respectively (*Nowlin and Zenk* [1988]; no ratios are given). The comparably low value in Drake Passage, even some years later, supports the notion (section 4)

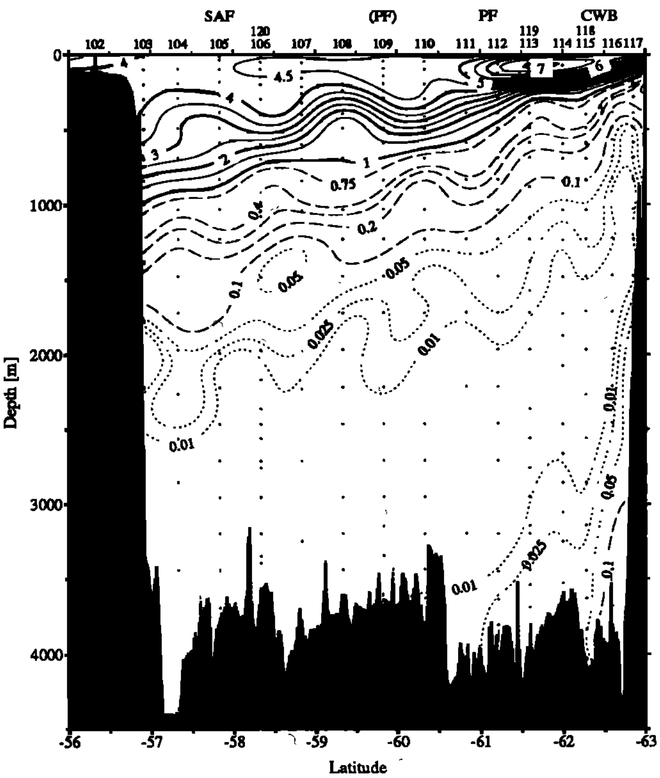

Fig. 5. *Meteor* CFM 11 section (picomoles per kilogram); see Figure 3. The two lowest contours shown (0.025 pmol/kg; 0.01 pmol/kg = detection limit) have considerable uncertainty.

that there is only moderate spreading of WSDW up to the *Meteor* section. The CFM 11 to CFM 12 ratio measured in the WSDW core is characteristic of surface waters in 1969, and the observed concentration is 8 times lower than that corresponding to this ratio (Figure 1). These values, following *Weiss et al.* [1985], yield for the ventilated component of the WSDW a tentative travel time to the *Meteor* section of 21 years (i.e., 1969-1990; upper limit, see section 2), and a dilution of least eightfold.

The detection limit isoline (0.01 pmol/kg) that marks the boundary of the deep CFM core is met inside the SEPDW (Table 1, Figure 3*e*). This suggests that any CFM that we observed in this water mass is primarily due to admixture from the WSDW, so that an original SEPDW contribution advected from the west would have to be small. An approximate upper limit for such contribution is believed to be 0.025 pmol/kg in CFM 11.

The next water mass upward, LCDW, has CFM 11 below the detection limit north of the PF (using the water mass definition of Table 1). South of the PF, the detection limit concentration penetrates into the high-salinity core (Figure 3*b*), and the maximum concentration, found at the upper LCDW boundary, still amounts to no more than about 1% of surface water concentrations. In total, CFM 11 is below, or near to, the detection limit over most of the LCDW. Thus the CFM distribution strongly supports low ventilation for the LCDW upstream of Drake Passage. We note that nonvanishing CFM 11 throughout the water column has been found in the Weddell Sea [*Foster and Weiss* [1988]; *Schlosser et al.* [1991]; unpublished *Meteor* 11 data southeast of the South Orkney Islands). LCDW being regarded as a major water source for this region (see introduction), it follows that this water mass must acquire CFMs downstream of Drake Passage, so that there is indication of an asymmetry in LCDW ventilation upstream and downstream of Drake Passage. It is noted that the CFM detection limit concentration north of the PF is found just below the 100–μmol/kg silica isoline, and south of the PF it coincides with the 110-μmol/kg isoline. To the degree that this correlation with silica is valid over a larger region, it could be useful to define an upper boundary of old waters whenever silica but not CFM data are available.

Across the UCDW (Table 1; Figure 3*e*) CFM 11 concentrations increase both upward and southward. Concentrations at the upper boundary in the very north of the section are near 10% of the local surface water concentration, rising to about 50% near the PF and further south. In the north, the detection limit concentration is near the center of the oxygen minimum (Figure 3*c*), consistent with the expectation that no significant ventilation from the north occurs. The CFM concentration at the southern tip of the 180-μmol/kg oxygen contour (Figure 3*c*, near station 118) amounts to approximately 0.5 pmol/kg, or 8% of surface water concentration (Figure 1). The concentration therefore corresponds to a contribution of ventilated water of approximately 10% if the transit time of this component from the surface is no more than a few years. In total, the CFM distribution indicates substantial ventilation of the UCDW from the south.

Figure 6 shows the CFM 11 to CFM 12 partial pressure ratios for the section, plotted versus CFM 11 partial pressure. There is indication of a small increase in ratios toward large CFM 11 values, but toward low CFM values, ratios remain essentially constant. It follows that the distributions of the two CFMs are very nearly the same. The ratios below 100-pptv partial pressure are incompatible with the relationship expected according to Figure 1 (regional tropospheric history or piston flow line; section 2), which is shown in Figure 6. This discrepancy indicates that effects of mixing are important (section 2, southern ocean case). The ratios at intermediate and higher CFM partial pressures are similar to values reported by *Gordon et al.* [1992, Figure 6] for the Cape Basin area. Of note in our Drake Passage observations, however, is the fact that a decline of ratios toward low partial pressures is barely present.

We pursue this finding further by simulating CFM distributions using a highly idealized model representing tracer transport in this regime. We reduce the problem to one dimension by considering transport to be predominantly isopycnal, and by projecting water trajectories on a meridional plane. This leads us to modeling transport as isopycnal advection along such a plane (velocity v) of CFM-free water from the north, and countermixing (apparent diffusivity K; v and K constant) from the southern outcrop of the isopycnal, the outcrop attaining CFM concentrations according to Figure 1. Advection will flush tracer back toward the outcrop, from where it was obtained previously by the mixing. Advection will thus assist the mixing in replacing tracer acquired previously by tracer of a more recent signature, i.e., CFM ratio. A time scale characteristic of this effect is $t^* = K/v^2$. In the limit that t^* is very much larger than a time typical of the CFM transient (on the order of 10 years; Figure 1), the CFM distribution along the isopycnal will be brought forth by mixing alone (pure mixing limit). For smaller t^*, flushing by advection will become noticeable, and ratios at low concentrations will be even higher.

CFM concentrations were simulated by running the advection-diffusion model forward in time over the period of the CFM transient up to 1990, starting from vanishing concentrations. Model results for two values of t^* are compared in Figure 7 with

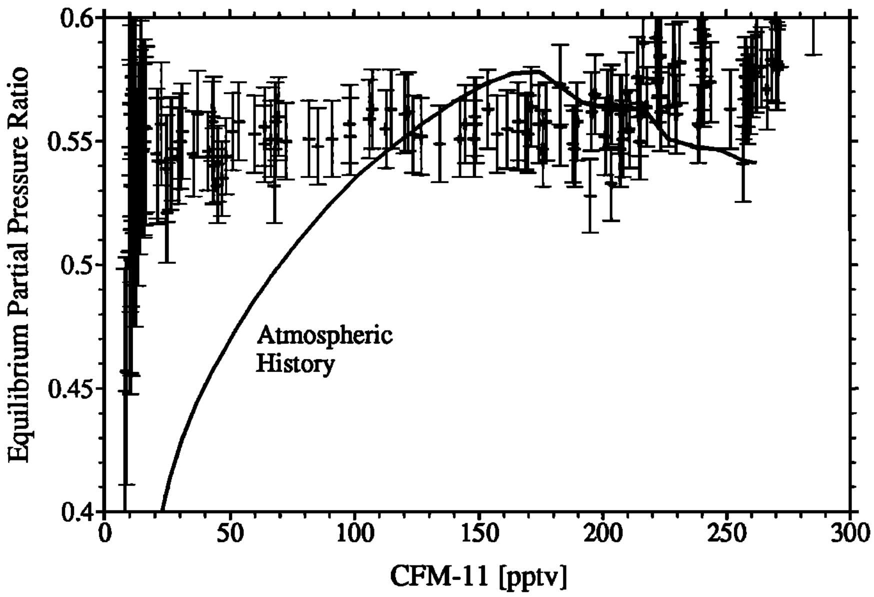

Fig. 6. CFM 11 to CFM 12 partial pressure ratio versus CFM 11 partial pressure for the data points of Figure 5. Bars indicate standard errors of ratios; data below 8 pptv in CFM 11 have been omitted, and a few outliers were removed. The relationship in ocean surface water as a function of time ("atmospheric history" or piston flow line, Figure 1) is shown for reference.

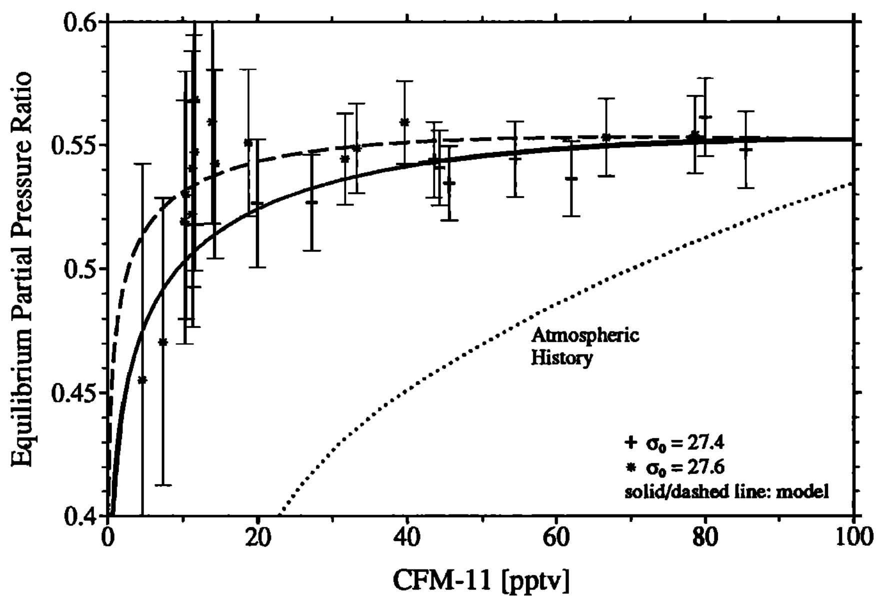

Fig. 7. Observed CFM 11 to CFM 12 partial pressure ratios versus CFM 11 partial pressure (between 8 and 90 pptv) on the isopycnals σ_0 = 27.4 (pluses) and 27.6 (asterisks), compared with curves from isopycnal advection/diffusion model (solid line, pure-mixing limit; dashed line, flushing time scale t^* = 30 years). For explanation see text; for atmospheric history curve see Figure 6.

CFM data interpolated to isopycnals representative of the UCDW (σ_0 = 27.4 and 27.6). The solid curve represents the pure mixing limit, and the dashed one, indicating stronger enhancement, a case in which advection begins to be effective. The agreement between model curves and data is gratifying. There is even a tendency for the shallower isopycnal to follow more closely the pure mixing case, and the deeper one the case with noticeable advection. Approximate model parameter values (obtained by fitting model curves to the observed mean northward decline in concentrations on the isopycnals in question, Figure 8) are K = 250 m^2/s (about the same for both model cases) and v = 15 km/yr (for the case with t^* = 30 years). Accounting for the average slope of the isopycnals in question (Figure 3*e*), the model advection corresponds to an approximate vertical upwelling velocity w = 40 m/yr. The values for K and w obtained are consistent with values in the literature [*Webb et al.*, 1991; *Gordon and Huber*, 1990; *Schlosser et al.*, 1987]. A general conclusion that can be drawn from the simulation is that in an upwelling regime such as the southern ocean, virtual absence of a decline in CFM 11 to CFM 12 ratios toward low CFM concentrations is a natural phenomenon. In such a situation, CFM 11 to CFM 12 ratios will cease to provide information on water "age".

6. Isopycnal Distributions and Property Transport

Figures 8*a* to 8*d* show CFM 11, oxygen, salinity, silica, and depth on density isolines versus latitude in the density range

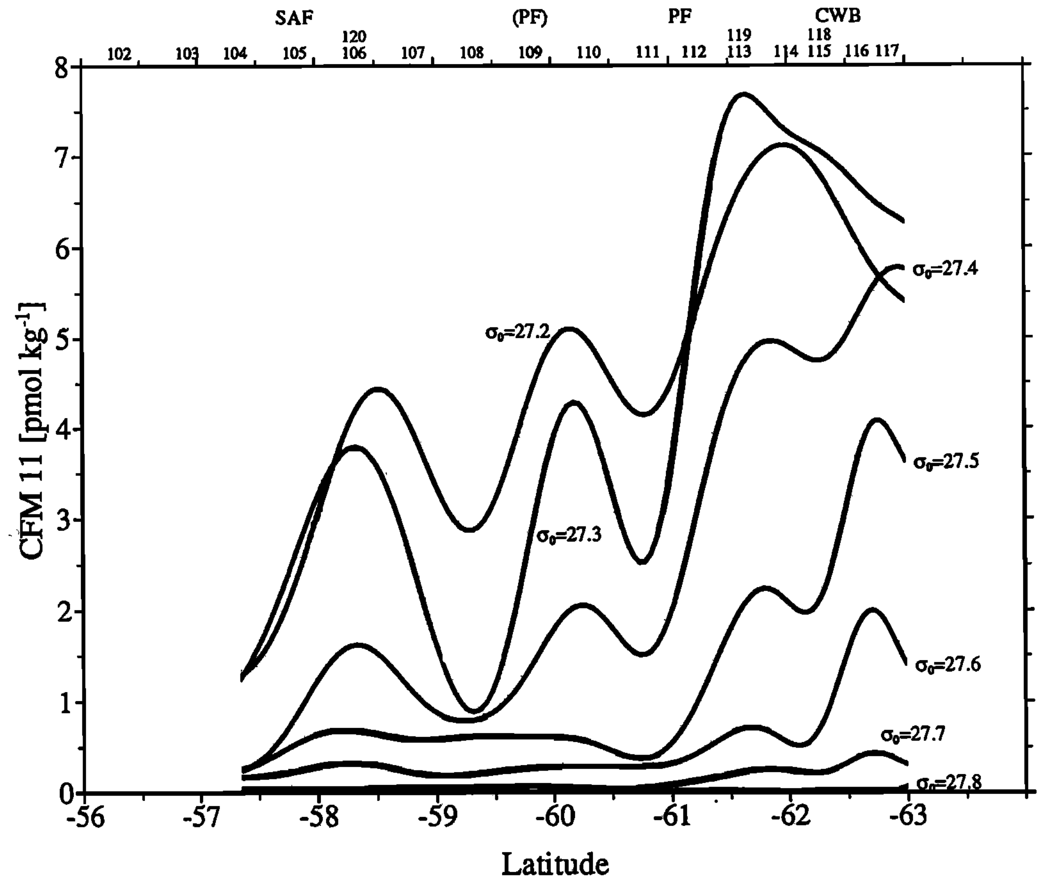

Fig. 8*a*. CFM 11 versus latitude on σ-isolines. Although depth partly exceeds 1000 m, σ_0 is displayed throughout for clarity; differences in slope relative to densities as in Figure 3*e* should remain small. For explanation see text.

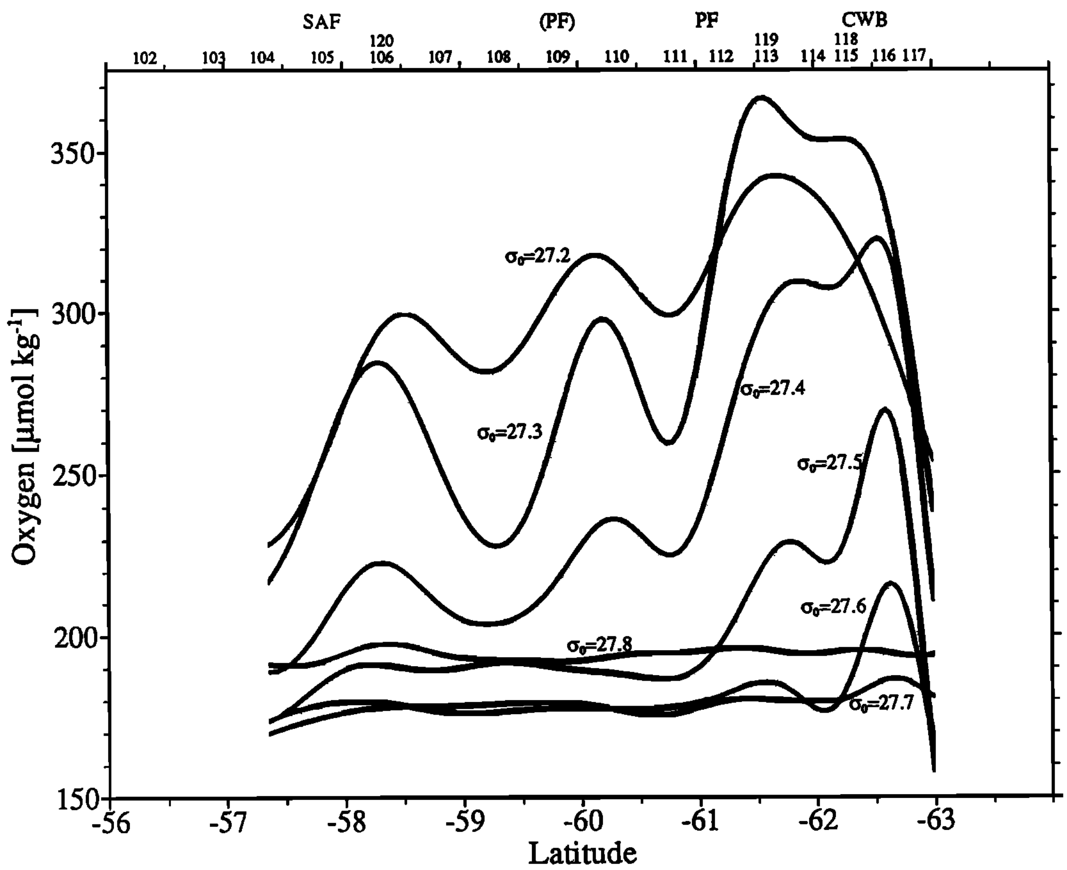

Fig. 8*b*. Same as Figure 8*a*, for oxygen versus latitude.

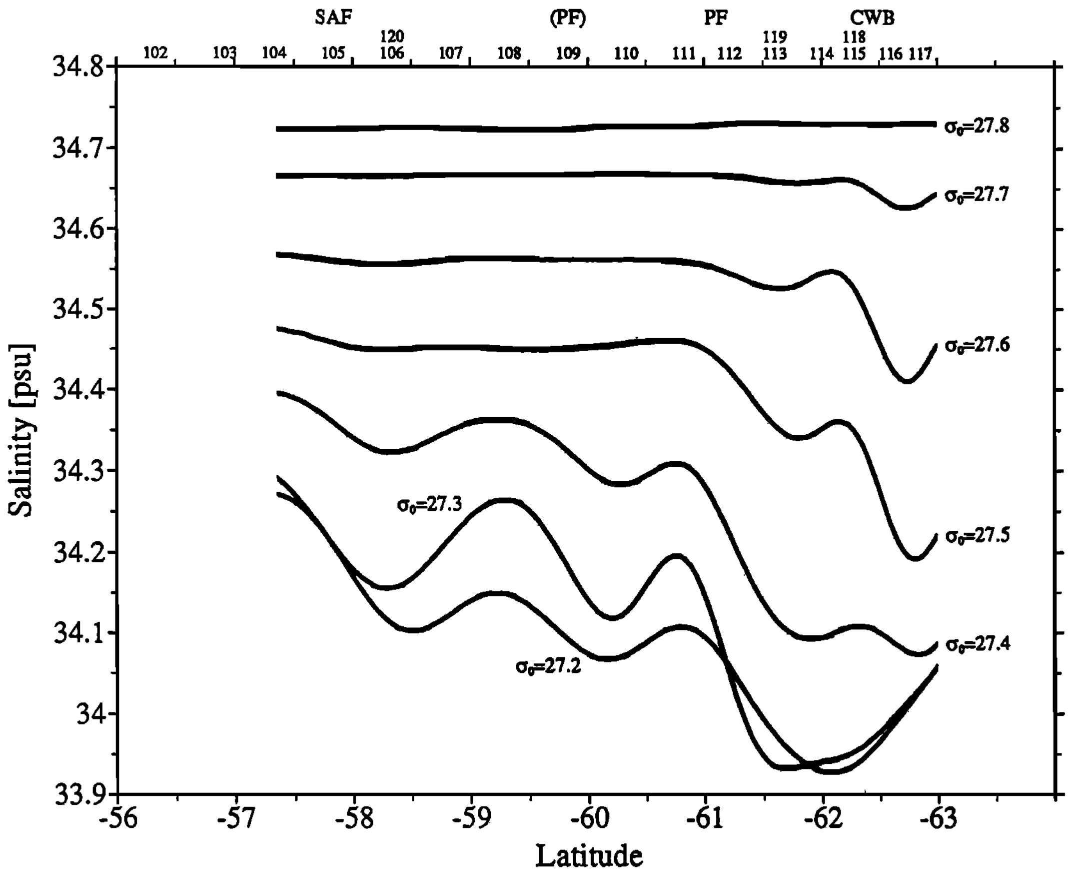

Fig. 8c. Same as Figure 8a, for salinity versus latitude.

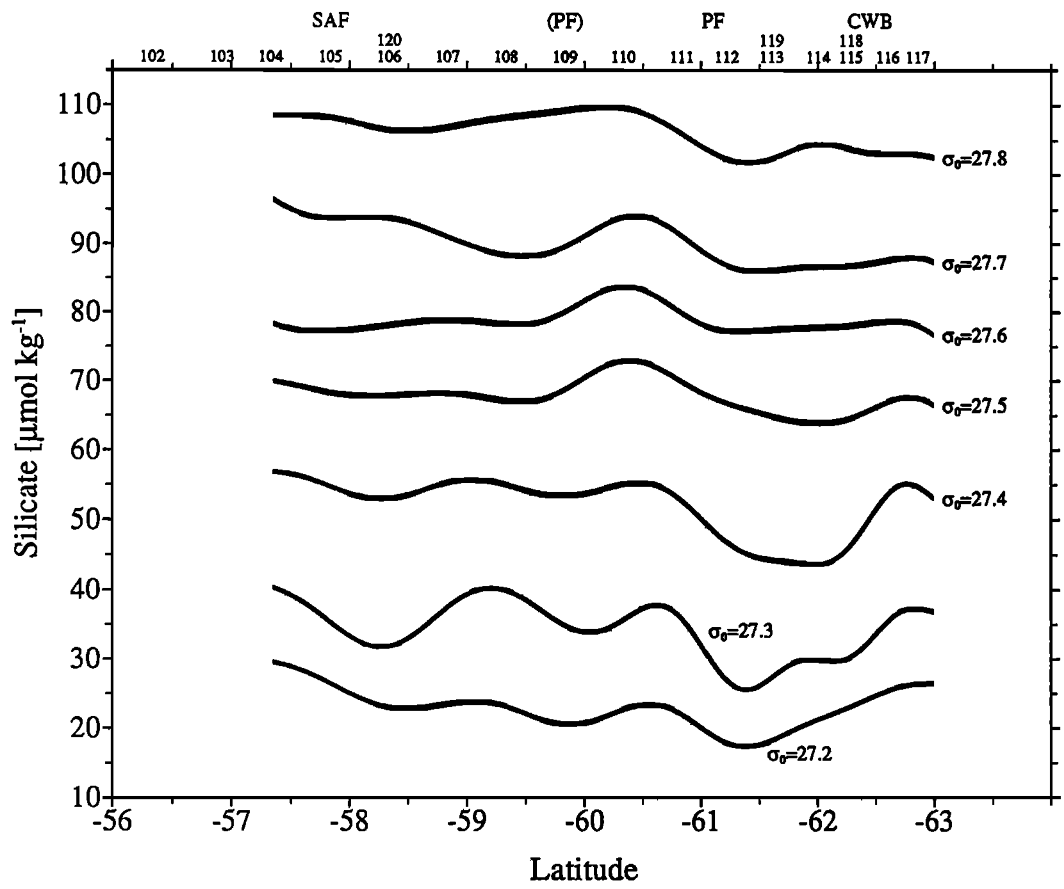

Fig. 8d. Same as Figure 8a, for silica versus latitude.

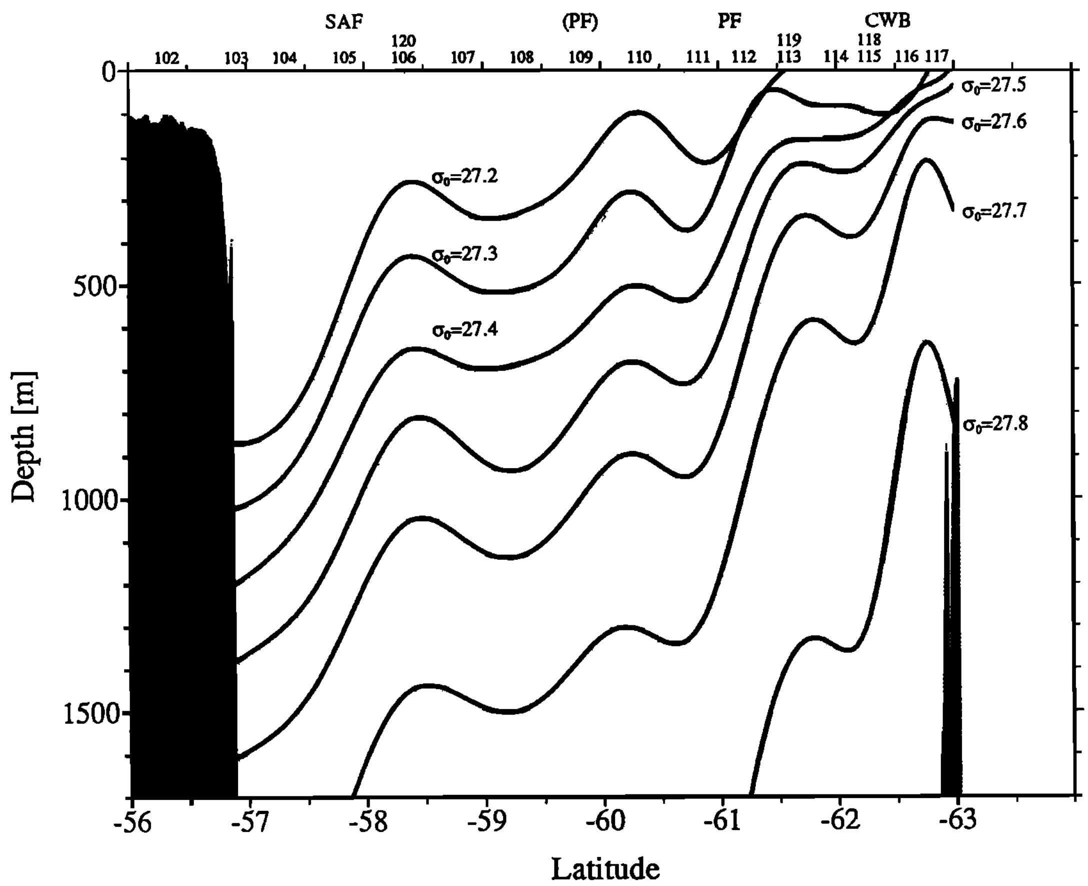

Fig. 8*e*. Same as Figure 8*a*, for depth versus latitude (see Figure 3*e*).

$\sigma_0 = 27.2$ to 27.8. The figures were constructed by objective interpolation with spatially variable correlation lengths adjusted subjectively, but for which the station distance and vertical data spacing were taken as lower bounds, and subsequent subsampling on isopycnals. Figure 8*a* exhibits a northward decrease of CFM 11 along isopycnals, on average, consistent with ventilation from the south, but with large undulations superimposed. Three maxima appear with a fourth one indicated near the southern end of the section; the two northern ones are similar in magnitude. The features become small at about the $\sigma_0 = 27.5$ isopycnal in the north (halfway into the UCDW) and at the 27.7 isopycnal south of the PF (approximately at the UCDW/LCDW boundary). They are thus restricted to about the upper 1000 m, similar to the case for the temperature undulations (Figure 3*a*) noted above.

Oxygen (Figure 8*b*) shows very similar undulations, apart from a more pronounced maximum near the southern margin. The similarity in detail even on the deeper isolines, where the variations are quite small, is intriguing. Also, salinity (Figure 8*c*), and to a lesser extent silica (Figure 8*d*), show surprisingly similar structure, low values being correlated with high CFM and oxygen. Such property correlation indicates that the extrema are due to larger and smaller contributions of young water of southern origin, respectively. The positions of the CFM 11 and oxygen maxima and minima along the section coincide with those in depth (Figure 8*e*). The extrema are thus found at the boundaries of the current bands related to the fronts of the ACC. The findings in Figure 8 can be summarized as enhanced north-south change in water characteristics on isopycnals across the fronts, and reversed gradients in between the fronts.

Across-ACC advection by rings is offered as an explanation that readily explains the findings. A possible scenario is that we happened to encounter rings, just at the said boundaries, that appeared there accidentally or by effect of local topographic steering. The CFM maxima would be related to cold-core rings that had broken off from a more southerly front and thus carried southerly water characteristics. The minima might be due to warm-core rings or, as such rings supposedly are relatively rare (see above), they might represent the background field. The facts that the features have been found on all of the current bands of the ACC, and that the related property changes are large, strongly support previous views [*Bryden*, 1983] that advection by rings is an important mechanism of property transport across the ACC. It is noted in passing that locally varying vertical admixture from above could hardly explain the findings, as the related variable bouyancy input would require compensating admixture of "older" water from below. Dominating vertical mixing would also contradict the basically lateral coherence of the water masses (Figure 3). Likewise, an effect of special trajectories within the ACC flow field that have particularly short or prolonged transit time from their outcrops is hardly plausible. Another point is that no extrema were observed below the UCDW, but this might be due to smaller variation in water characteristics across the ACC relative to the waters further up, so that rings would cease to generate significant differences in water characteristics.

The basic scenario of ring action might tentatively be developed further. Rings adhering to fronts of the ACC have been observed repeatedly and in various regions (see introduction). If attraction of rings to fronts is sufficiently strong, gradual degradation of the rings could result in bands along the fronts that have their water properties modified by the rings. The modification would be such that, as before, across-front property gradients would become enhanced, and possibly to a degree that gradients in between the fronts would be reversed. Velocities in the countercurrents in Figure 4 are relatively small compared with typical velocities of rings [*Bryden*, 1983], so that the *Meteor* observations are not inconsistent with the notion of a rather more continuous deposition process. If this modified scenario is true, it would naturally provide a baroclinic driving mechanism for the countercurrents between the frontal jets that have often been observed (see above). It would also lend support to the previous claim [*Lutjeharms*, 1989] that rings help to maintain the fronts by restoring the across-front gradient in dynamical height against the action of cross-frontal mixing.

7. Concluding Remarks

The close similarity noted (section 4) of the hydrographic and nutrient distributions in 1990 with those from the 1970s [*Sievers and Nowlin*, 1984], which indicates that temporal changes of water properties in Drake Passage are small, may not be surprising considering that the water masses involved mostly have rather long renewal time scales. Qualitative evidence on the renewal is provided by the observed CFM concentrations (section 5). For example, the UCDW/LCDW boundary north of the PF appears to be characterized by CFM concentrations falling below the detection limit, while south of the PF a limited CFM penetration into the LCDW is apparent. The implied ventilation of the LCDW in total remains small, but we concluded from literature data that LCDW ventilation should increase considerably downstream of Drake Passage. To allow a conversion of CFM information into water renewal rates (see section 2), more extended (in area or time, or including more transient tracers) observations and/or model studies, such as those to be provided by the WOCE program, are called for.

The observation that CFM 11 to CFM 12 ratios are essentially constant down to low CFM concentrations, and their successful simulation by a simple advection/diffusion model (section 5), both reveal that there are situations in which the ratio entirely loses its often quoted capability to be used as an "age" marker. The ratios remain nonredundant, but their evaluation now requires explicit treatment of circulation and mixing, i.e., a model approach.

It appears that the *Meteor* data provide the first detailed documentation of property extrema on isopycnal surfaces across the ACC. We ascribe these to the action of rings (section 6), notably cold-core rings depositing water of southern characteristics at the southern boundary of the fronts of the ACC. Our findings may be very special, but if the aforementioned features are a more general phenomenon (and for some reason so far escaped attention) they should be of considerable relevance for property transport across the ACC, and possibly for the energy budget of the fronts. We propose that dedicated observations and/or model studies be performed to decide the issue. The features are expected to carry a distinct transient-tracer signature. Field work should primarily consist of closely spaced observations across the ACC, but study of the along-ACC coherence of the features might also be advisable.

Acknowledgments. We are grateful to the master (H. Papenhagen) and crew of *Meteor* 11/5 for outstanding cooperation, and to the scientific party of the cruise for splendid assistance. Advice by W. D. Nowlin, Jr., Texas A&M University, during and after the cruise is particularly appreciated. We thank D. Olbers, Bremerhaven, for discussions; B. Ruddick, Halifax, and D. Wolf-Gladrow, Bremerhaven, for literature advice; and two anonymous reviewers for helpful suggestions. R. F. Weiss, La Jolla, kindly provided the CFM standard and tabulations of atmospheric CFM concentrations. The work was supported by grants received from the Deutsche Forschungsgemeinschaft and the Bundesminister für Forschung und Technologie, Bonn. AWI contribution 467.

References

Brickman, D., and B. Ruddick, The behavior and stability of a lens in a strain field, *J. Geophys. Res.*, *95*, 9657-9670, 1990.
Bryden, H. L., The southern ocean, in *Eddies in Marine Science*, edited by A. R. Robinson, pp. 265-277, Springer-Verlag, New York, 1983.
Bullister, J. L., and R. F. Weiss, Determination of CCl_3F and CCl_2F_2 in seawater and air, *Deep Sea Res.*, *35*, 839-853, 1988.
Doney, S. C., and J. L. Bullister, A chlorofluorocarbon section in the eastern North Atlantic, *Deep Sea Res.*, *39*, 1857-1883, 1992.
Emery, W. J., Antarctic polar frontal zone from Australia to the Drake Passage, *J. Phys. Oceanogr.*, *7*, 811-822, 1977.
Foster, T. D., and R. F. Weiss, Antarctic Bottom Water formation in the northwestern Weddell Sea, *Antarct. J. U.S.*, 74-76, 1988.
Gammon, R. H., J. Cline, and D. Wisegarver, Chlorofluoromethanes in the North Pacific ocean: Measured vertical distributions and application as transient tracers of upper ocean mixing, *J. Geophys. Res.*, *87*, 9441-9454, 1982.
GEOSECS, *GEOSECS Atlantic, Pacific and Indian Ocean Expeditions, Shorebased Data and Graphics, GEOSECS Atlas Ser.*, vol. 7, 200 pp., National Science Foundation, Washington, D.C., 1987.
Gordon, A. L., and B. A. Huber, Southern ocean winter mixed layer, *J. Geophys. Res.*, *95*, 11,655-11,672, 1990.
Gordon, A. L., and H. W. Taylor, Heat and salt balance within the cold waters of the world ocean, in *Numerical Models of Ocean Circulation*, pp. 54-56, National Academy of Sciences, Washington, DC, 1975.
Gordon, A. L., R. F. Weiss, W. M. Smethie, and M. J. Warner, Thermocline and intermediate water communication between the South Atlantic and Indian oceans, *J. Geophys. Res.*, *97*, 7223-7240, 1992.
Hofmann, E. E., and T. Whitworth III, A synoptic description of the flow at Drake Passage from year-long measurements, *J. Geophys. Res.*, *90*, 7177-7187, 1985.
Lutjeharms, J. R. E., The role of mesoscale turbulence in the Agulhas Current system, in *Mesoscale/Synoptic Coherent Structures in Geophysical Turbulence*, edited by J. C. J. Nihoul and B. M. Jamart, pp. 357-373, Elsevier Science, New York, 1989.
Lutjeharms, J. R. E., and H. R. Valentine, Southern ocean thermal fronts south of Africa, *Deep Sea Res.*, *31*, 1461-1475, 1984.
Nowlin, W. D., Jr., and J. M. Klinck, The physics of the Antarctic Circumpolar Current, *Rev. Geophys.*, *24*, 469-491, 1986.
Nowlin, W. D., Jr., and W. Zenk, Westward bottom currents along the margin of the South Shetland island arc, *Deep Sea Res.*, *35*, 269-301, 1988.
Nowlin, W. D., Jr., T. Whitworth III, and R. D. Pillsbury, Structure and transport of the Antarctic Circumpolar Current from short-term measurements, *J. Phys. Oceanogr.*, *7*, 788-802, 1977.
Pickart, R. S., N. G. Hogg, and W. M. Smethie, Jr., Determining the strength of the deep western boundary current using the chlorofluoromethane ratio, *J. Phys. Oceanogr.*, *19*, 940-951, 1989.
Reid, J. L., W. D. Nowlin, Jr., and W. C. Patzert, On the characteristics and circulation of the southwestern Atlantic Ocean, *J. Phys. Oceanogr.*, *7*, 62-91, 1977.
Roether, W., M. Samthein, T. J. Müller, W. Nellen, and D. Sahrhage, Südatlantik-Zirkumpolarstrom, Reise Nr. 11, 3. Oktober 1989 - 11. März 1990, *Meteor*-Ber. 90-2, 169 pp, Univ. Hamburg, Hamburg, Germany, 1990.
Schlosser, P., W. Roether, and G. Rohardt, ^{3}He balance of the upper layers of the northwestern Weddell Sea, *Deep Sea Res.*, *34*, 365-377, 1987.
Schlosser, P., J. L. Bullister, and R. Bayer, Studies of deep water formation and circulation in the Weddell Sea using natural and anthropogenic tracers, *Mar. Chem.*, *35*, 97-122, 1991.
Sievers, H. A., and W. J. Emery, Variability of the Antarctic Polar Frontal Zone in the Drake Passage: Summer 1976-1977, *J. Geophys. Res.*, *83*, 3010-3022, 1978.
Sievers, H. A., and W. D. Nowlin, Jr., The stratification and water masses at Drake Passage, *J. Geophys. Res.*, *89*, 10,489-10,514, 1984.
Sievers, H. A., and W. D. Nowlin, Jr., Upper ocean characteristics in Drake Passage and adjoining areas of the southern ocean, 39°W-95°W, in *Antarctic Ocean and Resources Variability*, edited by D. Sahrhage,

pp. 57-80, Springer-Verlag, New York, 1988.
Smith, D. C., and G. P. Davis, Jr., A numerical study of eddy interaction with an ocean jet, *J. Phys. Oceanogr.*, *19*, 975-986, 1989.
Stern, M. E., and G. R. Flierl, On the interaction of a vortex with a shear flow, *J. Geophys. Res.*, *92*, 10,733-10,744, 1987.
Stuiver, M., P. D. Quay, and H. G. Ostlund, Abyssal water carbon-14 distributions and the age of the world oceans, *Science*, *219*, 849-851, 1983.
Warner, M. J., and R. F. Weiss, Solubilities of chlorofluorocarbons 11 and 12 in water and seawater, *Deep Sea Res.*, *32*, 1485-1497, 1985.
Webb, D. J., P. D. Killworth, A. C. Coward, and S. R. Thompson, *The FRAM Atlas of the Southern Ocean*, 67 pp., Natural Environmental Research Council, Swindon, England, 1991.
Weiss, R. F., J. L. Bullister, R. H. Gammon, and M. J. Warner, Atmospheric chlorofluoromethanes in the deep equatorial Atlantic, *Nature*, *314*, 608-610, 1985.
Whitworth, T., III, and W. D. Nowlin, Jr., Water masses of the southern ocean at the Greenwich meridian, *J. Geophys. Res.*, *92*, 6462-6476, 1987.
World Climate Research Program (WCRP), World Ocean Circulation Experiment implementation plan, vol. I, Detailed requirements, *WCRP-11*, p. 2-2, World Meteorol. Organ., Geneva, July 1988*a*.
WCRP, World Ocean Circulation Experiment implementation plan, vol. II, Scientific background, *WCRP-12*, p. 3-6, World Meteorol. Organ., Geneva, July 1988*b*.

P. Beining, K. Bulsiewicz, A. Putzka, W. Roether, and R. Schlitzer, Universität Bremen, Fachbereich 1, D-28334 Bremen, Germany.
F. Delahoyde, ODF, Scripps Institution of Oceanography, La Jolla, CA 92093.
G. Rohardt, Alfred-Wegener-Institut für Polar- und Meeresforschung, D-27515 Bremerhaven, Germany.

(Received December 30, 1991;
revised September 3, 1992;
accepted December 31, 1992.)